Am J Physiol Heart Circ Physiol 300: H514–H521, 2011.
First published November 12, 2010; doi:10.1152/ajpheart.00814.2010.

The thermodynamics of diastole: kinematic modeling-based derivation of the P-V loop to transmitral flow energy relation with in vivo validation

Sina Mossahebi,[3] Leonid Shmuylovich,[2] and Sándor J. Kovács[1,2,3]

[1]*Cardiovascular Biophysics Laboratory, Cardiovascular Division,* [2]*Division of Biology and Biomedical Sciences, School of Medicine, and* [3]*Department of Physics, College of Arts and Sciences, Washington University, St. Louis, Missouri*

Submitted 16 August 2010; accepted in final form 11 November 2010

Mossahebi S, Shmuylovich L, Kovács SJ. The thermodynamics of diastole: kinematic modeling-based derivation of the P-V loop to transmitral flow energy relation with in vivo validation. *Am J Physiol Heart Circ Physiol* 300: H514–H521, 2011. First published November 12, 2010; doi:10.1152/ajpheart.00814.2010.—Pressure-volume (P-V) loop-based analysis facilitates thermodynamic assessment of left ventricular function in terms of work and energy. Typically these quantities are calculated for a cardiac cycle using the entire P-V loop, although thermodynamic analysis may be applied to a selected phase of the cardiac cycle, specifically, diastole. Diastolic function is routinely quantified by analysis of transmitral Doppler E-wave contours. The first law of thermodynamics requires that energy (ε) computed from the Doppler E-wave ($\varepsilon_{E\text{-wave}}$) and the same portion of the P-V loop ($\varepsilon_{P\text{-V E-wave}}$) be equivalent. These energies have not been previously derived nor have their predicted equivalence been experimentally validated. To test the hypothesis that $\varepsilon_{P\text{-V E-wave}}$ and $\varepsilon_{E\text{-wave}}$ are equivalent, we used a validated kinematic model of filling to derive $\varepsilon_{E\text{-wave}}$ in terms of chamber stiffness, relaxation/viscoelasticity, and load. For validation, simultaneous (conductance catheter) P-V and echocadiographic data from 12 subjects (205 total cardiac cycles) having a range of diastolic function were analyzed. For each E-wave, $\varepsilon_{E\text{-wave}}$ was compared with $\varepsilon_{P\text{-V E-wave}}$ calculated from simultaneous P-V data. Linear regression yielded the following: $\varepsilon_{P\text{-V E-wave}} = \alpha\varepsilon_{E\text{-wave}} + b$ ($R^2 = 0.67$), where $\alpha = 0.95$ and $b = 6e^{-5}$. We conclude that E-wave-derived energy for suction-initiated early rapid filling $\varepsilon_{E\text{-wave}}$, quantitated via kinematic modeling, is equivalent to invasive P-V-defined filling energy. Hence, the thermodynamics of diastole via $\varepsilon_{E\text{-wave}}$ generate a novel mechanism-based index of diastolic function suitable for in vivo phenotypic characterization.

diastolic function; pressure-volume loop; echocardiography

DIASTOLIC DYSFUNCTION is a predictor of, and a precursor to, diastolic heart failure, or heart failure with normal ejection fraction (EF), a growing clinical syndrome that has reached epidemic proportions (17, 24, 41). Critical to the diagnosis and management of diastolic heart failure is quantitative diastolic function assessment. Although left ventricular (LV) hemodynamics constitute the gold standard for characterizing diastolic function, echocardiography remains the preferred method clinically. Acknowledged limitations of current echo-derived clinical diastolic function indexes justify the continued quest for novel, physiological, mechanism-based rather than merely echocardiographic waveform phenomenology-based diastolic function indexes that correlate with dysfunction.

In previous work, we have developed and validated novel mechanism-based indexes of diastolic function via a kinematic modeling approach, called the parameterized diastolic filling (PDF) formalism (13, 19, 20). The PDF formalism models the kinematics of suction-initiated filling as the recoil, from rest, of an equivalent damped oscillator. Model-predicted velocity and clinical E-wave contours have shown superb agreement. Using any clinically recorded E-wave as input and suitable mathematical methods, unique chamber stiffness (k), viscoelasticity/relaxation (c), and load (x_o) parameters are generated as output, thereby solving the "inverse problem of diastole" (13). The three PDF parameters (k, c, and x_o) can be used to generate indexes with rigorous physiological analogs, such as the peak instantaneous pressure gradient (kx_o), among others (1).

Although previous work has shown that subjects with diastolic dysfunction may have stiffer chambers (30) or altered values for chamber viscoelasticity/relaxation (30) relative to controls, the physiology of diastole, and early rapid filling in particular, has not been fully elucidated in thermodynamic terms. Indeed, while both systolic and diastolic energies may be calculated from pressure-volume (P-V) loops, it is not known whether P-V loop-derived measures of energy have a direct noninvasive E-wave-derived analog. Thus, in this work, we derived an E-wave-based expression for the energy associated with early rapid filling and hypothesized that, in accordance with the first law of thermodynamics, the energy of filling computed from Doppler echocardiography (a relative measure) should be linearly related to energy calculated from simultaneously acquired P-V data (an absolute measure).

METHODS

Patient Selection

Data sets from 12 patients (mean age: 64 yr, 8 men and 4 women) were selected from our existing cardiovascular laboratory database of simultaneous echocardiographic high-fidelity hemodynamic (Millar conductance catheter) recordings (6, 22). Subjects underwent elective cardiac catheterization to determine the presence of coronary artery disease at the request of their referring physicians. The data selection criteria for the study included a broad range of LV end-diastolic pressures (LVEDP) representative of a patient population encountered clinically, normal LV EF (>50%), normal sinus rhythm, clearly discernible E-waves followed by a diastatic interval, and normal valvular function. Before data acquisition, subjects provided signed Institutional Review Board-approved informed consent for participation in accordance with Washington University Human Research Protection Office-approved criteria. The method of simultaneous echocardiographic transmitral flow and P-V data recording is well established and has been previously detailed (3, 21, 23). Among the 12 data sets, 5 data sets had LVEDP < 15 mmHg, 4 data sets had 15 mmHg < LVEDP < 20 mmHg, and 3 data sets had LVEDP > 20 mmHg. A total of 205 cardiac cycles of simultaneous echocardiographic high-fidelity hemodynamic (conductance catheter) data was analyzed. The clinical descriptors of the 12 subjects and their hemodynamic and echocardiographic indexes are shown in Table 1.

Address for reprint requests and other correspondence: S. J. Kovács, Cardiovascular Biophysics Laboratory, Washington Univ. Medical Center, 660 S. Euclid Ave., Box 8086, St. Louis, MO. 63110 (e-mail: sjk@wuphys.wustl.edu).

Table 1. *Clinical descriptors of the 12 subjects including hemodynamic and echocardiographic indexes*

Parameter	
No. of subjects	12
Age, yr	64 ± 13
Sex (men/women)	8/4
Heart rate, beats/min	62 ± 8
LV ejection fraction, %	75 ± 12
LV end-diastolic pressure, mmHg	18 ± 6
LV end-diastolic volume, ml	145 ± 35
Pressure at diastasis, mmHg	15 ± 5
E/*A*	2.2 ± 0.7
Parameterized diastolic filling parameters	
Load (x_o), cm	9.3 ± 4.6
Chamber stiffness (k), 1/s^2	211 ± 84
Viscoelasticity/relaxation (c), 1/s	17.3 ± 12

Values are means ± SD. The left ventricular (LV) ejection fraction was determined by ventriculography. *E*/*A*, ratio of the peak E-wave to peak A-wave.

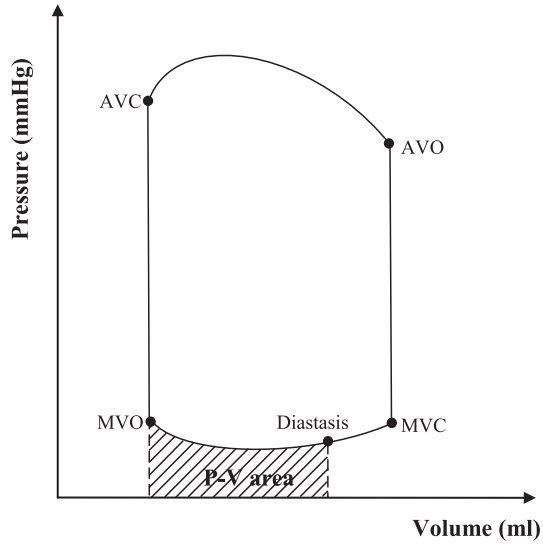

Fig. 1. Schematic pressure-volume (P-V) loop defining the P-V area as a measure of energy, from mitral valve opening (MVO) to diastasis, encompassing the suction-initiated early rapid filling (Doppler E-wave) interval. AVC, aortic valve closure; AVO, aortic valve opening; MVC, mitral valve closure. See text for details.

Data Acquisition

The simultaneous high-fidelity, P-V, and echocardiographic transmitral flow data recording method has been previously detailed (3, 21, 23). Briefly, LV pressure and volume were acquired using micromanometric conductance catheter (SPC-560, SPC-562, or SSD-1043, Millar Instruments, Houston, TX) at the commencement of elective cardiac catheterization before the administration of iodinated contrast agents. Pressure signals from the transducers were fed into a clinical amplifier system (Quinton Diagnostics, Bothell, WA, and General Electric). Conductance catheterization signals were fed into a custom personal computer via a standard interface (Sigma-5, CD Leycom). Conductance-volume data were recorded in five channels. Data from low-noise channels providing physiological readings were selected, suitably averaged, and calibrated using absolute volumes obtained by calibrated ventriculography during the same procedure.

Doppler E-Wave Analysis

For each subject, ~1–2 min of continuous transmitral flow data were recorded in the pulsed-wave Doppler mode. Echocardiographic data acquisition was performed in accordance with published American Society of Echocardiography (27) criteria. Briefly, immediately before catheterization, patients are imaged in a supine position using a Philips (Andover, MA) iE33 system. Two-dimensional images in apical two- and four-chamber views were obtained. In accordance with convention, the apical four-chamber view was used for Doppler E-wave recording with the sample volume located at the leaflet tips. Averages of 17 beats/subject were analyzed (205 cardiac cycles total for the 12 subjects). All E-waves were analyzed via PDF formalism (see APPENDIX A) via model-based image processing to yield E-wave-specific kinematic parameters (k, c, and x_o) (19, 21).

Hemodynamic Analysis

Hemodynamics were determined from the high-fidelity Millar LV pressure and volume data from each beat. A custom MATLAB program was used to find the end-systolic and diastatic P-V data points. Diastatic points were defined by ECG P-wave onset, and, according to convention, mitral valve opening pressure on the continuous LV pressure tracing was estimated to be equal to LVEDP (4, 15, 25, 26).

Definition of the P-V Area During the E-Wave

The diastolic P-V area, as shown in Fig. 1, represents the work done by the recoiling chamber during early rapid filling (E-wave). This area was computed numerically from P-V data directly and was defined in the P-V plane as the area under the P-V curve from mitral valve opening to diastasis.

Derivation and Calculation of the Kinematic Energy

For a damped simple harmonic oscillator, with spring constant k and initial displacement x_o recoiling from rest, the potential energy before recoil is $1/2kx_o^2$. Because the oscillator is damped, only a fraction of the total potential energy is available as external work during the E-wave. Work is defined as $\int F\mathrm{d}x$, where F is force and $\mathrm{d}x$ is displacement. By expressing the result in terms of PDF parameters, we obtain the following:

$$\int \mathrm{Fd}x = \left(\frac{1}{2}kx_o^2\right)\mathrm{KFEI} \qquad (1)$$

where the kinematic filling efficiency index (KFEI; always <1) is the proportionality constant that determines what fraction of the total potential energy $1/2kx_o^2$ is delivered as external $\{F\mathrm{d}x\}$ work (38).

To gain more insight into the physiological determinants of E-wave energy and since the PDF formalism provides closed-form algebraic expression for transmitral flow velocity [$v(t)$] as a function of time, we expressed LV pressure in terms of $v(t)$ and acceleration [$\mathrm{d}v(t)/\mathrm{d}t$] using Bernoulli's equation for nonsteady flow (35, 37). We obtained the area under the E-wave portion of the P-V loop by integrating the Bernoulli equation-derived expression for LV pressure (P) in $\int \mathrm{PdV}$, as a function of volume (V), from mitral valve opening to diastasis. This yielded the following expression for diastolic kinematic energy ($\varepsilon_{\text{E-wave}}$) in terms of PDF parameters (c, k, and x_o):

$$\varepsilon_{\text{E-wave}} = \rho \times \mathrm{MVA}\left(\frac{1}{2}kx_o^3\right)\left[\frac{4}{3} + \left(\frac{\sqrt{k}}{2c}\right)\exp\left(-\frac{3c\mathrm{DT}}{2}\right)\right] + C' \qquad (2)$$

where ρ is the density of blood, MVA is the effective (constant) mitral valve area, DT is the deceleration time of the E-wave, and C' is the constant of integration. For simplicity, MVA was constant (4 cm^2) and ρ was 1.060 g/ml. See APPENDIX B for mathematical details.

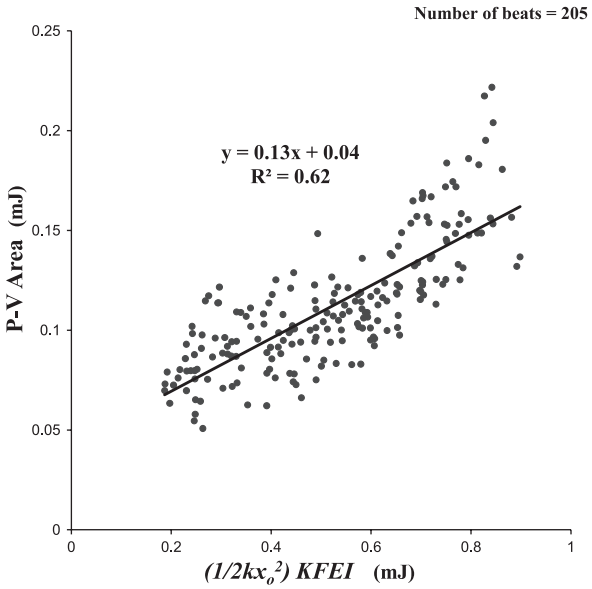

Fig. 2. Correlation between the experimentally measured P-V area as the ordinate and E-wave-determined potential energy ($1/2kx_o^2 \times$ KFEI, where k is chamber stiffness, x_o is load, and KFEI is the kinematic filling efficiency index) as the abscissa. See text for details.

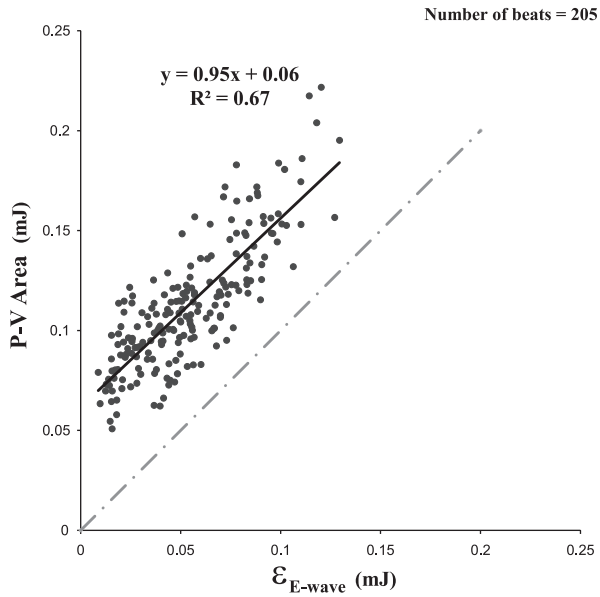

Fig. 3. Correlation between the experimentally measured P-V area as the ordinate and model-predicted kinematic energy ($\varepsilon_{E\text{-wave}}$) as the abscissa. See text for details.

RESULTS

P-V Area Versus Energy as (1/2kx$_o^2$)KFEI

The P-V area and potential energy of the damped simple harmonic oscillator were highly correlated ($R^2 = 0.62$) for all analyzed beats (Fig. 2).

When analyzed on an individual basis, the high correlation between P-V area and potential energy ($R^2 > 0.69$) was maintained. Individual linear regression for each data set is shown in Table 2. We compared potential energy versus the P-V area (as the reference). ANOVA-derived P values of <0.05 were considered statistically significant.

P-V Area Versus Kinematic Energy $\varepsilon_{E\text{-wave}}$

In accordance with the derivation, the P-V area and kinematic energy $\varepsilon_{E\text{-wave}}$ were highly correlated ($R^2 = 0.67$) for all analyzed beats (Fig. 3). When analyzed individually, data for all 12 subjects showed that the P-V area strongly correlated with kinematic energy ($R^2 > 0.60$). Individual linear regressions for the subjects are shown in Table 3. For all subjects, kinematic energy versus the P-V area, analyzed using ANOVA, yielded P values of <0.05 and were statistically significant.

DISCUSSION

Echocardiography is the preferred method of diastolic function assessment. To provide a more complete set of causality-based diastolic function indexes, we used thermodynamic principles. We determined the E-wave-derived analog of invasively measured (P-V loop derived) diastolic energy. While stroke work is a familiar energy-based index, the energy associated with diastolic recoil, a necessary component for total energy balance, has not been fully appreciated. Elastic

Table 2. *Individual least-mean-square linear regression slopes and intercepts for pressure-volume area-derived versus kinematic model-derived potential energy expressed as (1/2kx$_o^2$)KFEI for 12 subjects*

Subject	Linear Fit Slope	Linear Fit Intercept	R^2 Value
1	0.03	2 *e*−3	0.79
2	0.05	1 *e*−4	0.75
3	0.09	1 *e*−1	0.83
4	0.12	2 *e*−2	0.80
5	0.02	6 *e*−2	0.77
6	0.05	2 *e*−2	0.75
7	0.06	3 *e*−2	0.81
8	0.04	4 *e*−2	0.83
9	0.03	5 *e*−2	0.76
10	0.06	2 *e*−2	0.69
11	0.07	3 *e*−2	0.87
12	0.03	4 *e*−2	0.77

KFEI, kinematic filling efficiency index.

Table 3. *Individual least-mean-square linear regression slopes and intercepts for pressure-volume area versus kinematic energy $\varepsilon_{E\text{-wave}}$ (Eq. 2) incorporating the Bernoulli equation and near-constant volume physiology for 12 subjects*

Subject	Linear Fit Slope	Linear Fit Intercept	R^2 Value
1	0.92	5 *e*−2	0.69
2	1.19	5 *e*−2	0.67
3	1.69	9 *e*−5	0.85
4	3.58	2 *e*−2	0.78
5	0.62	7 *e*−2	0.80
6	1.41	4 *e*−2	0.77
7	1.46	4 *e*−2	0.60
8	1.20	6 *e*−2	0.88
9	0.57	8 *e*−2	0.69
10	1.76	5 *e*−2	0.69
11	1.50	4 *e*−2	0.87
12	0.74	6 *e*−2	0.79

$\varepsilon_{E\text{-wave}}$, energy computed from the Doppler E-wave.

strain energy, stored during the prior systole, is unmasked during relaxation and drives diastolic recoil. It results in the mechanical suction of atrial blood by generating an atrioventricular pressure gradient resulting in the E-wave (12, 14, 16, 29). Using complementary methods and mathematical modeling, we derived two expressions for diastolic energy in terms of parameters obtained from the E-wave alone. We tested the validity of our derived energy expressions for the same physiological event by determining the correlation between values obtained using simultaneous invasive (P-V loop) versus noninvasive (echo) data in 12 subjects. In accordance with thermodynamic requirements, we found a strong correlation. This represents the first study where expressions for diastolic energy have been derived from first principles and validated using simultaneous invasive and noninvasive data acquisition methods.

Thermodynamics and the Heart

The total LV generated external work (stoke work) per cardiac cycle (in J) is given by $\int$PdV around the P-V loop. The systolic P-V area, a measure of total mechanical energy generated by ventricular contraction, closely correlates with cardiac O_2 consumption under a variety of loading conditions for a given contractile (inotropic) state (32–34). Similarly, the tension-time integral or force-time integral (11) can convey work done by the chamber. Efficiency of the chamber has been computed as the ratio of output or external work (in J) divided by input (myocardial O_2 consumption) (18). These measurements typically yield an efficiency of ~25%. Instead of the entire cycle, we consider the external work during diastole, since diastolic energy, a component of $\int$PdV, has not, to our knowledge, ever been specifically calculated or analyzed.

By considering the early rapid filling phase of diastole, we define the diastolic P-V area as the measure of external work done by the chamber during the E-wave. We obtained this experimentally from the area of the P-V loop ($\int$PdV) from mitral valve opening to diastasis (see Fig. 1). This area represents the absolute (invasive) measure of external PdV work of the chamber during the E-wave ($\varepsilon_{\text{P-V E-wave}}$).

An independent transmitral flow-based relative measure of E-wave energy can be obtained via kinematic modeling of suction-initiated filling ($\varepsilon_{\text{E-wave}}$). Thermodynamic laws require that relative and absolute measurements of the same event be linearly related and differ by a constant of integration (C').

KFEI

Systole stores elastic strain energy (potential energy), which is unmasked by relaxation and powers the mechanical recoil/ventricular suction process. The PDF formalism provides a simple expression, $1/2kx_o^2$, for energy available to power an idealized, lossless, and symmetric (about its peak) E-wave. However, actual E-waves must be asymmetric, and the extent of asymmetry reflects filling-related energy losses. We have previously computed KFEI as actual E-wave volume (parameterized by x_o, c, and k) divided by the maximum possible (idealized) E-wave volume, parameterized by identical x_o and k but generated in the absence of viscous losses ($c = 0$ kinematics) (38). KFEI therefore incorporates viscous losses/relaxation effects associated with the balance between chamber damping (c) and chamber stiffness (k).

The KFEI differentiated E-waves of normal LV EF diabetic hearts from E-waves of normal LV EF nondiabetic controls more robustly than traditional clinical parameters such as deceleration time (38). KFEI's connection to E-wave energy provides valuable insights into the current work. In analogy to KFEI, the potential energy of the oscillator ($1/2kx_o^2$) can also be considered in the ideal lossless ($c = 0$) setting and the actual in vivo ($c \neq 0$) setting. In the lossless setting, KFEI = 1, all of the oscillator's potential energy is converted to kinetic energy (velocity), and no energy is lost as viscous dissipation. In the actual in vivo setting, some energy is always lost to dissipation, and only a fraction of the initial $1/2kx_o^2$ energy is delivered as the kinetic energy of filling. Because KFEI is a dimensionless index of kinematic filling efficiency, it is appropriate to estimate the actual delivered energy powering filling as the product of KFEI and ideal energy powering filling ($1/2kx_o^2$).

Theoretical P-V Loop

Using the nonsteady Bernoulli equation and PDF formalism-derived expressions for flow (E-wave) velocity [$v(t)$] and acceleration [$dv(t)/dt$], expressions for LV pressure and volume as a function of time can be derived. Eliminating time provides pressure as a function of volume. This yields kinematic and fluid mechanics-based modeling-derived algebraic expressions for the early filling portion of the P-V loop in terms of PDF parameters (k, c, and x_o). To find the area under the P-V loop during early filling, the derived P(V) expression is integrated from mitral valve opening to diastasis, coinciding with E-wave duration.

In previous work we have modeled the P-V loop kinematically and demonstrated that the model-derived analog of maximum elastance (E_{max}) was a function only of intrinsic model parameters rather than initial conditions, and, therefore, the analogous E_{max} relationship was load independent (28). However, that approach relied on modeling the entire cardiac cycle. In this work we instead focused on the early rapid filling-related portion of the P-V loop, and we did this by applying the nonsteady Bernoulli equation.

Application of the Nonsteady Bernoulli Equation

Previous work has demonstrated the importance of including both convective and inertial terms in the Bernoulli equation when modeling transmitral flow (9). By approximating the inertial term as the product of mitral inertiance and acceleration and applying the proper limit, we are able to derive an expression for the atrioventricular pressure gradient in terms of PDF parameters (*Eq. B6*). In constructing a P-V loop from this expression, we treated the atrial pressure term as an unknown constant to extract ventricular pressure alone. This introduces a systematic offset in our final expression and in the area under the theoretically constructed P-V loop. Thus, the nonzero asymptote shown in Fig. 3 is primarily the result of treating the atrial pressure term as an unknown constant. This linear offset is the expected consequence of comparing an absolute catheterization-based measure (P-V area) to a relative measure (theoretical P-V loop area derived from the E-wave alone), and the correlation shown in Fig. 3 is expected to be stronger and have an intercept closer to zero if the atrial pressure recording was available and contributed to ΔP in the construction of the

final expression. The value of the intercept shown in Fig. 3 was consistent across subjects (see Table 3).

Determining Diastolic Recoil Energy in the Context of "Absolute" Versus "Relative" Measurement

Diastolic recoil energy from the P-V loop shown graphically in Fig. 1 can be computed in alternate ways. For the P-V loop shown in Fig. 1, atmospheric zero is, by convention, the fiducial reference. However, for the E-wave-derived expression for energy (see *Eq. B12*), the offset relative to atmospheric zero or any fiducial value cannot be specified (it is C' in *Eq. B12*).

Indeed, when we compared diastolic recoil energies determined from the invasive (an "absolute" measure) and noninvasive (a "relative" measure) approaches (Fig. 3), we observed a nonzero intercept. The nonzero intercept is the experimental equivalent of C' in *Eq. B12* in APPENDIX B. It is the result of the alternate choice of atmospheric zero versus mean atrial pressure or diastatic pressure as the reference fiducial pressure relative to which energy variation is computed. Using the diastatic P-V curve as a reference constitutes another option (39). We tested the extent to which choice of fiducial pressure (atmospheric vs. zero reference) affects the regression between E-wave-derived and P-V-derived energies. The correlations between kinematic energy using zero as the constant of integration versus actual P-V area were unaltered. Therefore, the observed offset introduced by the choice of reference pressure has no effect on the expected linear correlation between invasive ("absolute") versus noninvasive ("relative") measures of recoil energies.

Future Studies

This initial work is focussed on deriving and validating the predicted relationship between invasive and noninvasive measures of diastolic energy. Broader clinical application should include a spectrum of suitably selected pathophysiological states such as heart failure with normal EF, hypertension, diabetes, infiltrative disease, etc. Furthermore, energy-based indexes are suitable for studies where each subject serves as their own control and the response to selected therapies for diastolic dysfunction are assessed using conventional methods and in terms of repeated measures of recoil energy. Although expected to be load dependent, diastolic recoil energy indexes can be trended in concert with a previously derived and validated load-independent index of diastolic function obtained by suitable analysis of the E-wave (31).

Limitations

Conductance volume. The conductance catheter method of volume determination has known limitations related to noise, saturation, and calibration that we have previously acknowledged (1, 3, 22). In this study, the channels that provided physiologically consistent P-V loops were selected and averaged. However, since there was no significant drift of volume signal during recording, any systematic offset related to calibration of the volume channels did not affect the result when the limits of conductance volume were calibrated via quantitative ventriculography.

P-V measurements. Our assumption that mitral valve opening pressure approximates LVEDP has limitations. It has been shown (36) that this assumption is valid in the setting of normal physiology. In an abnormal case (abnormal valve function and LV EF) where mitral valve opening pressure and end-diastolic pressure are significantly different, the use of end-diastolic pressure in the P-V area will introduce a systematic error but will still represent a reasonable estimate of energy during early filling; it will also affect the offset of the correlation of P-V area and $\varepsilon_{E\text{-wave}}$. To minimize any systematic difference between mitral valve opening pressure and LVEDP in our analysis of 205 heart beats in 12 subjects, we selected data sets only for subjects with normal valve function and normal LV EF (4, 15, 26, 40).

E-wave selection. Although the PDF formalism is applicable to all E-waves, the most robust analysis is achieved for E-waves that have a clear termination and are followed by diastasis. E-wave analysis becomes less reliable when the A-wave merges with the E-wave and covers more than two-thirds of the E-wave deceleration portion. This typically occurs at heart rates of >90 beats/min (2). In the present study, we used data sets with clearly discernible E-waves followed by a diastatic interval (average heart rate = 62 beats/min).

Choosing the limits of the integral in Bernoulli's equation. We assumed simultaneous E-wave and E′-wave onsets in deriving kinematic energy (see APPENDIX B). It is possible that some E′-waves are slightly delayed (by a few milliseconds) beyond E-wave onsets (5). For simplicity and consistency and for ease of the integration, we assumed that E′-wave duration and deceleration time are comparable. This assumption only affects the magnitude of $\varepsilon_{E\text{-wave}}$ for every single beat and has no significant effect on the slope and correlation between $\varepsilon_{P\text{-}V\ E\text{-wave}}$ and $\varepsilon_{E\text{-wave}}$.

Application of Bernoulli's equation. In deriving the expression for kinematic energy ($\varepsilon_{E\text{-wave}}$), we applied a form of Bernoulli;s equation for an ideal fluid, where fluid viscosity is ignored. This approach has been applied by previous investigators (35, 37), and studies have demonstrated its validity (8, 9). Recall that the PDF model (damped oscillation) accounts for energy loss in kinematic terms via the parameter c; hence, by using the PDF-derived expression for velocity in the Bernoulli equation, we automatically include the effects of losses in the system (damping) as part of the kinetic energy term in the Bernoulli equation. In effect the expression for fluid velocity and acceleration includes the parameter c and therefore already includes energy losses as part of the resulting expression for pressure. This insures that energy conservation is maintained in accordance with Bernoulli's law and includes the dominant form of energy loss due to kinematic modeling-derived viscoelastic losses rather than (negligible) fluid viscosity losses.

Sample size. The number of data sets (n = 12) is a minor limitation to the study, because the total number of cardiac cycles analyzed (n = 205) mitigates it to an acceptable degree.

Conclusions

By deriving thermodynamics-based and kinematic modeling-based expressions for the work of suction-initiated filling (E-wave) and using in vivo, human, simultaneous P-V and transmitral echocardiographic data for validation, we showed (to within an additive constant of integration) the predicted equivalence between echo-derived (relative)

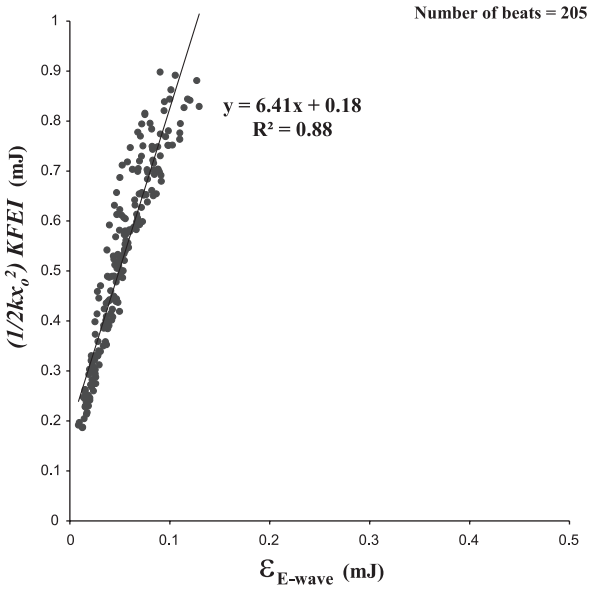

Fig. 4. Correlation between potential energy ($1/2kx_o^2 \times$ KFEI) and kinematic energy $\varepsilon_{E\text{-}wave}$ (theoretical P-V area). See text for details.

and P-V loop-derived (absolute) measures of diastolic energy. These results establish energy ($1/2kx_o^2$) as a legitimate, mechanism-based, echo-derived diastolic function index obtainable via kinematic modeling-based analysis of clinically recorded E-waves. Figs. 4 and 5.

APPENDIX A

Simultaneous Acquisition of Echocardiographic and High-Fidelity Hemodynamic Data

Before arterial access, in the catheterization laboratory, a full two-dimensional echo-Doppler study was performed by an American Society of Echocardiography-certified sonographer in accordance with American Society of Echocardiography criteria (27). After an appropriate sterile skin preparation and drape, local anaesthesia (1% xylocaine) was given, and percutaneous right or left femoral arterial access was obtained in preparation for catheterization and angiography using a valved sheath (6-F, Arrow, Reading, PA). After arterial access and placement of a 64-cm sheath (Arrow), a 6-Fr micromanometer-tipped pigtail (triple pressure transducer) P-V conductance catheter (models 560-1 or 560-5, Millar Instruments, Houston, TX) was directed into the mid-LV in a retrograde fashion across the aortic valve under fluoroscopic control. Before insertion, the manometer-tipped catheter was calibrated against "zero" by submersion just below the surface of a normal saline bath at 37°C and again after insertion relative to hydrostatic "zero" using the lumen with respect to the midthoracic fluid-filled transducer (HP). It was balanced using a transducer control unit (model TC-510, Millar Instruments), and pressure was fed to the catheterization laboratory amplifier (Quinton Diagnostics, Bothell, WA, or GE Healthcare, Milwaukee, WI) and simultaneously into the input ports of the physiological amplifier of the Doppler imaging system for synchronization (iE33, Philips). With the patient in the supine position, apical four-camber views using a 2.5-MHz transducer were obtained by the sonographer, with the sample volume gated at 1.5–5 mm directed between the tips of the mitral valve leaflets and orthogonal to the mitral valve plane. Continuous wave Doppler was used to record aortic outflow and mitral inflow from the apical view for the determination of isovolumic relaxation time using a sweep speed of 10 cm/s. Doppler tissue imaging of the medial and lateral mitral annulus and M-mode images were also recorded. To synchronize the hemodynamic data with the Doppler data, a fiducial marker in the form of a square wave was fed from the catheter-transducer control unit. LV and aortic pressure, LV volume from the conductance catheter, and one ECG channel were also simultaneously recorded on disk. Simultaneous Doppler data, LV pressure, and conductance volume were obtained for a minimum of 30 consecutive heart beats during quiet respiration. After data acquisition, the diagnostic catheterization procedure was performed in the usual manner.

PDF Formalism

PDF formalism models the kinematics of early rapid LV filling in analogy to the motion of a damped simple harmonic oscillator (19, 40). The governing equation of motion is as follows:

$$m\frac{d^2x}{dt^2} + c\frac{dx}{dt} + kx = 0 \qquad (A1)$$

The formalism solves the "inverse problem" by providing (mathematically) unique parameters c, k, and x_o that determine each Doppler E-wave contour (19, 20, 40). The initial displacement of the oscillator x_o (in cm) is linearly related to the E-wave velocity-time integral (i.e., a measure of volumetric preload) and chamber stiffness ($\Delta P/\Delta V$) is linearly related to the model's spring constant k (in g/s^2) while the oscillator's damping constant or chamber viscoelasticity/relaxation index c (in g/s) characterizes the resistance (relaxation/viscosity) and energy loss associated with filling (20, 40). E-waves with long concave up deceleration portions ("delayed relaxation pattern") have high c values, whereas E-waves that approximate symmetric sine waves have low c values. The contour of the clinical E-wave is predicted by the (underdamped) solution for the velocity of a damped oscillator, given by the following:

$$v(t) = -\frac{x_o k}{\omega}\exp(-ct/2)\sin(\omega t) \qquad (A2)$$

where $\omega = \sqrt{4mk - c^2}/2m$.

PDF parameter values for c, k, and x_o were determined using the Levenberg-Marquardt algorithm to fit to the E-wave maximum velocity envelope via a custom LabView (National Instruments, Austin, TX) interface (3, 7, 20, 30, 40). By setting mass $m = 1$, we can calculate the parameters per unit mass.

APPENDIX B

Derivation of Kinematic Energy

To incorporate the near perfect constant-volume attribute of the four-chambered and two- chambered heart, left heart atrioventricular

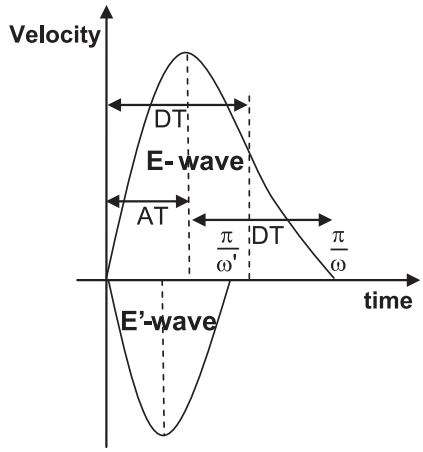

Fig. 5. Schematic diagrams showing the E-wave and E′-wave. AT, acceleration time; DT, deceleration time. See text for details.

external geometry was modeled as a right circular cylinder having a fixed height (L) and fixed cross-sectional area (A). It was subdivided into upper and lower chambers representing the left atrium (LA) and LV, respectively.

v_E and $v_{E'}$ are the Doppler-derived mitral inflow velocity and Doppler tissue imaging-recorded mitral annulus velocity. With the constraint that LV mass is conserved between systole and diastole and noting that the combined atrial and ventricular blood volume remains essentially constant between systole and diastole, we obtain the following (10):

$$\mathrm{MVA} \times v_E = A \times v_{E'} \tag{B1}$$

The volume of the heart and volume of the LV (V_{LV}) can be written as $A \times L$ and $L \times x$, respectively. By taking derivative of LV volume and using *Eq. B1*, we obtain the following:

$$dV_{LV} = A \times dx = A \times v_{E'} dt = \mathrm{MVA} \times v_E dt \tag{B2}$$

The following relation between kinematic energy $\varepsilon_{E\text{-wave}}$ and PDF parameters can be derived from Bernoulli's equation for nonsteady flow:

$$\Delta P = \mathrm{LAP} - \mathrm{LVP} = \frac{1}{2}\rho v_E^2 + \rho \int_{LA}^{LV} \frac{\partial v(s,t)}{\partial t} ds \tag{B3}$$

where LAP is LA pressure, LVP is LV pressure, and s is distance along a streamline.

The integral can be rewritten as $M(dv_E/dt)$, where M (a constant) is the mitral inertiance (35, 37, 40). *Equation B3* thus becomes the following:

$$\mathrm{LVP} = -\frac{1}{2}\rho v_E^2 - M\frac{dv_E}{dt} + \mathrm{LAP} \tag{B4}$$

where M can be obtained by noting that at t = deceleration time (DT), the time of pressure crossover, LAP = LVP (40). Thus,

$$\Delta P = 0 = \frac{1}{2}\rho v_E^2\Big|_{t=DT} + M\frac{dv_E}{dt}\Big|_{t=DT}$$

$$M = -\frac{\frac{1}{2}\rho v_E^2\Big|_{t=DT}}{\frac{dv_E}{dt}\Big|_{t=DT}} = \frac{1}{2}\rho x_o\left(\frac{\sqrt{k}}{c}\right)\exp\left(-\frac{c\,DT}{2}\right) \tag{B5}$$

where

$$DT = \frac{\pi}{\omega} - \frac{1}{\omega}\arctan\left(\frac{2\omega}{c}\right)$$

By substituting $y = c(2\sqrt{k})$, LVP at any time t (*Eq. B4*) is as follows:

$$\mathrm{LVP} = -\frac{1}{2}\rho\left(v_E(t)^2 + x_o\left(\frac{1}{2y}\right)\exp\left\{-\frac{y\left[\pi - \cos^{-1}(y)\right]}{\sqrt{1-y^2}}\right\}\dot{v}_E(t)\right) + \mathrm{LAP} \tag{B6}$$

By integrating *Eq. B6* over V_{LV}, we can derive the P-V area (kinematic energy $\varepsilon_{E\text{-wave}}$) in term of PDF parameters. The result is as follows:

$$\varepsilon_{E\text{-wave}} = \int_{V(0)}^{V(\frac{\pi}{\omega})} \mathrm{LVP} \times dV_{LV} = -\frac{1}{2}\rho\int_{V(0)}^{V(\frac{\pi}{\omega})}\left(v_E(t)^2 + x_o\left(\frac{1}{2y}\right)\exp\left\{-\frac{y\left[\pi - \cos^{-1}(y)\right]}{\sqrt{1-y^2}}\right\}\dot{v}_E(t)\right) \times dV_{LV} + \underbrace{\int_{V(0)}^{V(\frac{\pi}{\omega})} \mathrm{LAP} \times dV_{LV}}_{C'} \tag{B7}$$

Since dV_{LV} was originally equal to $A \times v_{E'}dt$, limits can be determined by the duration of the E′-wave [$0 - (\pi/\omega')$] and LAP is treated as a constant of integration:

$$\varepsilon_{E\text{-wave}} = -\frac{1}{2}\rho\int_0^{\frac{\pi}{\omega}}\left(v_E(t)^2 + x_o\left(\frac{1}{2y}\right)\exp\left\{-\frac{y\left[\pi - \cos^{-1}(y)\right]}{\sqrt{1-y^2}}\right\}\dot{v}_E(t)\right) \times \mathrm{MVA} \times v_E(t)dt + C' \tag{B8}$$

$$\varepsilon_{E\text{-wave}} = -\frac{1}{2}\rho \times \mathrm{MVA}\left(\int_0^{\frac{\pi}{\omega}} v_E(t)^3 dt + x_o\left(\frac{1}{2y}\right)\exp\left\{-\frac{y\left[\pi - \cos^{-1}(y)\right]}{\sqrt{1-y^2}}\right\}\int_{v_E(0)}^{v_E(\frac{\pi}{\omega'})} v_E(t)dv_E\right) + C' \tag{B9}$$

where v_E, the E-wave velocity from PDF model, is given by $v(t) = -(x_o k/\omega)\exp(-ct/2)\sin(\omega t)$.

Since the specific relation between E-wave and E′-wave (see Fig. 5) PDF parameters depends on chamber geometry, the useful approximation for the upper limit of both integrals is t = DT, the time of E-wave inflection. After taking the integrals, we obtain the following:

$$\varepsilon_{E\text{-wave}} = \rho \times \mathrm{MVA}\left(\frac{1}{2}kx_o^3\right)\left[\frac{4}{3(1+8y^2)}\left[1 - y(5+8y^2)\right]\exp\left[-\frac{3y\arctan\left(\frac{\sqrt{1-y^2}}{y}\right)}{\sqrt{1-y^2}}\right] + \left(\frac{1}{4y}\exp\left\{-\frac{3y\left[\pi - \cos^{-1}(y)\right]}{\sqrt{1-y^2}}\right\}\right)\right] + C' \tag{B10}$$

For E-waves whose contours are well fit by the underdamped oscillation regime ($\sqrt{4k - c^2} > 0$) or $y < 1$, the equation becomes the following:

$$\varepsilon_{E\text{-wave}} \approx \rho \times \mathrm{MVA}\left(\frac{1}{2}kx_o^3\right)\left(\frac{4}{3} + \frac{1}{4y}\exp\left\{-\frac{3y\left[\pi - \cos^{-1}(y)\right]}{\sqrt{1-y^2}}\right\}\right) + C' \tag{B11}$$

This expression in terms of PDF parameters is:

$$\varepsilon_{E\text{-wave}} \approx \rho \times \mathrm{MVA}\left(\frac{1}{2}kx_o^3\right)\left[\frac{4}{3} + \left(\frac{\sqrt{k}}{2c}\right)\exp\left(-\frac{3c\,DT}{2}\right)\right] + C' \tag{B12}$$

ACKNOWLEDGMENTS

The authors thank sonographer Peggy Brown for expert echocardiographic data acquisition and the staff of the Cardiac Catheterization Laboratory (Cardiovascular Procedure Center, Barnes-Jewish Hospital) for assistance.

DISCLOSURES

No conflicts of interest, financial or otherwise, are declared by the author(s).

REFERENCES

1. **Bauman L, Chung CS, Karamanoglu M, Kovács SJ.** The peak atrioventricular pressure gradient to transmitral flow relation: kinematic model

prediction with in vivo validation. *J Am Soc Echocardiogr* 17: 839–844, 2004.
2. **Cheng C, Igarashi Y, Little W.** Mechanism of augmented rate of left ventricular filling during exercise. *Circ Res* 70: 9–19, 1992.
3. **Chung CS, Ajo DM, Kovács SJ.** Isovolumic pressure-to-early rapid filling decay rate relation: model-based derivation and validation via simultaneous catheterization echocardiography. *J Appl Physiol* 100: 528–534, 2006.
4. **Chung CS, Karamanoglu M, Kovács SJ.** Duration of diastole and its phases as a function of heart rate during spine bicycle exercise. *Am J Physiol Heart Circ Physiol* 287: H2003–H2008, 2004.
5. **Chung CS, Kovács SJ.** Consequences of increasing heart rate on deceleration time, velocity time integral and *E*/*A*. *Am J Cardiol* 47: 398–402, 2006.
6. **Chung CS, Kovács SJ.** Physical determination of left ventricular isovolumic pressure decline: model prediction with in vivo validation. *Am J Physiol Heart Circ Physiol* 294: H1589–H1596, 2008.
7. **Dent CL, Bowman AW, Scott MJ, Allen JS, Lisauskas JB, Janif M, Wickline SA, Kovács SJ.** Echocardiographic characterization of fundamental mechanisms of abnormal diastolic filling in diabetic rats with a parameterized diastolic filling formalism. *J Am Soc Echocardiogr* 14: 1166–1172, 2001.
8. **Falsetti HL, Verani MS, Chen CJ, Cramer JA.** Regional pressure differences in the left ventricle. *Catheter Cardiovasc Diag* 6: 123–134, 1980.
9. **Firstenberg MS, Vandervoort PM, Greenberg NL, Smedira NG, McCarthy PM, Garcia MJ, Thomas JD.** Noninvasive estimation of transmitral pressure drop across the normal mitral valve in humans: importance of convective and inertial forces during left ventricular filling. *J Am Coll Cardiol* 36: 1942–1949, 2000.
10. **Ghosh E, Shmuylovich L, Kovács SJ.** Determination of early diastolic LV vortex formation time (T*) via the PDF formalism: a kinematic model of filling. *Conf Proc IEEE Eng Med Biol Soc* 2009: 2883–2886, 2009.
11. **Goto Y, Slinker BK, LeWinter MM.** Decreased contractile efficiency and increased nonmechanical energy cost in hyperthyroid rabbit heart: relation between O_2 consumption and systolic pressure-volume area or force-time integral. *Circ Res* 66: 999–1011, 1990.
12. **Granzier H, Labeit S.** Cardiac titin: an adjustable multi-functional spring. *J Physiol* 541: 335–342, 2002.
13. **Hall AF, Kovács SJ.** Automated method for characterization of diastolic transmitral Doppler velocity contours: early rapid filling. *Ultrasound Med Biol* 20: 107–116, 1994.
14. **Helmes M, Trombitas K, Granzier H.** Titin develops restoring force in rat cardiac myocytes. *Circ Res* 79: 619–626, 1996.
15. **Ishida Y, Meisner J, Tsujioka K, Gallo J, Yoran C, Frater R, Yellin E.** Left ventricular filling dynamics: influence of left ventricular relaxation and left atrial pressure. *Circulation* 74: 187–196, 1986. [Erratum. Circulation 74(3): 462, 1986.]
16. **Jöbsis PD, Ashikaga H, Wen H, Rothstein EC, Horvath KA, McVeigh ER, Balaban RS.** Visceral pericardium: macromolecular structure and contribution to passive mechanical properties of the left ventricle. *Am J Physiol Heart Circ Physiol* 293: H3379–H3387, 2007.
17. **Kass DA, Bronzwaer JGF, Paulus WJ.** What mechanism underline diastolic dysfunction in heart failure? *Circ Res* 94: 1533–1542, 2004.
18. **Knaapen P, Germans T.** Myocardial efficiency in heart failure: non invasive imaging. *Heart Metab* 39: 14–19, 2008.
19. **Kovács SJ, Barzilai B, Pérez JE.** Evaluation of diastolic function with Doppler echocardiography: the PDF formalism. *Am J Physiol Heart Circ Physiol* 252: H178–H187, 1987.
20. **Kovács SJ, Meisner JS, Yellin EL.** Modeling of diastole. *Cardiol Clin* 18: 459–487, 2000.
21. **Kovács SJ, Sester R, Hall AF.** Left ventricular chamber stiffness from model-based image processing of transmitral Doppler E-waves. *Cor Art Dis* 8: 179–187, 1997.
22. **Lisauskas JB, Singh J, Courtois M, Kovács SJ.** The relation of the peak Doppler E-wave to peak mitral annulus velocity ratio to diastolic function. *Ultrasound Med Biol* 27: 499–507, 2001.
23. **Lisauskas JB, Singh J, Bowman AW, Kovács SJ.** Chamber properties from transmitral flow: prediction of average and passive left ventricular diastolic stiffness. *J Appl Physiol* 91: 154–162, 2001.
24. **Maeder MT, Kaye DM.** Heart failure with normal left ventricular ejection fraction. *J Am Coll Cardiol* 53: 905–918, 2009.
25. **Miki S, Murakami T, Iwase T, Tomita T, Nakamura Y, Kawai C.** Doppler echocardiographic transmitral peak early velocity does not directly reflect hemodynamic changes in humans. *J Am Coll Cardiol* 17: 1507–1516, 1991.
26. **Murakami T, Hess O, Gage J, Grimm J, Krayenbuehl H.** Diastolic filling dynamics in patients with aortic stenosis. *Circulation* 73: 1162–1174, 1986.
27. **Nagueh SF, Appleton CP, Gillebert TC, Marino PN, Oh JK, Smiseth OA, Waggoner AD, Flachskampf FA, Pellikka PA, Evangelista A.** Recommendations for the evaluation of left ventricular diastolic function by echocardiography. *J Am Soc Echocardiogr* 22: 107–133, 2009.
28. **Oommen B, Karamanoglu M, Kovács SJ.** Modeling time varying elastance: the meaning of "load-independence". *Cardiovasc Eng* 3: 123–130, 2003.
29. **Robinson TF, Factor SM, Sonnenblick EH.** The heart as a suction pump. *Sci Am* 254: 84–91, 1986.
30. **Riordan MM, Chung CS, Kovács SJ.** Diabetes and diastolic function: stiffness and relaxation from transmitral flow. *Ultrasound Med Biol* 31: 1589–1596, 2005.
31. **Shmuylovich L, Kovács SJ.** A load-independent index of diastolic filling: model-based derivation with in vivo validation in control and diastolic dysfunction subjects. *J Appl Physiol* 101: 92–101, 2006.
32. **Suga H, Goto Y, Futaki S, Kawaguchi O, Yaku H, Hata K, Takasago T.** Systolic pressure-volume area (PVA) as the energy of contraction in Starling's law of the heart. *Heart Vessels* 6: 65–70, 1991.
33. **Suga H.** Cardiac energetics: from E_{MAX} to pressure-volume area. *Clin Exp Pharmacol Physiol* 30: 580–585, 2003.
34. **Suga H.** Theoretical analysis of a left-ventricular pumping model based on the systolic time-varying pressure/volume ratio. *IEEE Trans Biomed Eng* 24: 29–38, 1977.
35. **Thomas JD, Newell JB, Choong CY, Weyman AE.** Physical and physiological determinants of transmitral velocity: numerical analysis. *Am J Physiol Heart Circ Physiol* 260: H1718–H1731, 1991.
36. **Wu Y, Kovács SJ.** Frequency-based analysis of the early rapid filling pressure-flow relation elucidates diastolic efficiency mechanisms. *Am J Physiol Heart Circ Physiol* 291: H2942–H2949, 2006.
37. **Yellin EL.** Mitral valve motion, intracardiac dynamics and flow pattern modelling: physiology and pathophysiology. In: *Advances in Cardiovascular Physics,* edited by Ghista DN. Basel: Karger, 1983, p. 137–161.
38. **Zhang W, Chung CS, Riordan MM, Wu Y, Shmuylovich L, Kovács SJ.** The kinematic filling efficiency index of left ventricle: contrasting normal vs. diabetic physiology. *Ultrasound Med Biol* 33: 842–850, 2007.
39. **Zhang W, Kovács SJ.** The diastatic pressure-volume relationship is not the same as the end-diastolic pressure-volume relationship. *Am J Physiol Heart Circ Physiol* 294: H2750–H2760, 2008.
40. **Zhang W, Shmuylovich L, Kovács SJ.** The E-wave delayed relaxation pattern to LV pressure contour relation: model-based prediction with in vivo validation. *Ultrasound Med Biol* 36: 497–511, 2010.
41. **Zile MR, Brutsaert DL.** New concepts in diastolic dysfunction and diastolic heart failure: part I. *Circulation* 105: 1387–1393, 2002.